22 September 1995

ELSEVIER

Chemical Physics Letters 243 (1995) 564–570

CHEMICAL
PHYSICS
LETTERS

Large rotational energy release in collision-induced SiF $C\,^2\Delta$–$B\,^2\Sigma^+$ valence–Rydberg transfer

Neil A. Jackson, Cameron W. Watson, Kenneth G. McKendrick *

Department of Chemistry, The University of Edinburgh, The King's Buildings, Edinburgh EH9 3JJ, UK

Received 19 June 1995; in final form 10 July 1995

Abstract

Distinct rotational population distributions were prepared in SiF $C\,^2\Delta$, $v = 0$ radicals by laser excitation. Collisions with H_2 or N_2 transferred a fraction of the $C\,^2\Delta$ molecules to the lower-lying $B\,^2\Sigma^+$ state. B–X fluorescence spectra revealed the nascent rotational populations in the predominant $B\,^2\Sigma^+$, $v' = 0$ level. An unusually large fraction of the available energy is released as SiF rotation, supplementing the initial SiF rotational angular momentum. There is greater SiF $B\,^2\Sigma^+$ product rotation for N_2 than for H_2. A simple impulsive model is capable of rationalising these observations, consistent with previous vibrationally resolved measurements and the valence-Rydberg character of the transition.

1. Introduction

Although the collisional quenching of electronically excited states of small molecules has been widely studied, in the great majority of cases only the total removal rates have been determined. It is much less common for the fate of the quenched molecules to be established.

Systems for which the vibronic products have been determined include N_2^+ $A\,^2\Pi_u$–$X\,^2\Sigma_g^+$ [1–3]; N_2 $B\,^3\Pi_g$–$B'\,^3\Sigma_u^-$ [4]; CH $A\,^2\Delta$–$B\,^2\Sigma^-$ [5,6]; OH $A\,^2\Sigma^+$–$X\,^2\Pi$ [7]; NH $c\,^1\Pi$–$A\,^3\Pi$ and $a\,^1\Delta$–$X\,^3\Sigma^-$ [8–10]; O_2 $b\,^1\Sigma_g^+$–$a\,^1\Delta_g$ [11]; NS $B\,^2\Pi$–$B'\,^2\Sigma^+$ and $B\,^2\Pi$–$b\,^4\Sigma^-$ [12]; NO $a\,^4\Pi$–$b\,^4\Sigma^-$ and $a\,^4\Pi$–$B\,^2\Pi$ [13]; and SiCl $B'\,^2\Delta$–$B\,^2\Sigma^+$ [14,15]. No clear picture has emerged of the critical properties of the initial and final states of the molecule, or indeed of the quencher, which control the branching between available vibrational levels. There is debate about the role of factors such as energy gaps: it is often assumed and has sometimes, but certainly not always, been observed that the dominant channels are those which are most nearly isoenergetic [1–4,12]. The influence of Franck–Condon overlap between initial and final vibrational wavefunctions is similarly unclear [2,3,10].

Not surprisingly, there have been even fewer determinations of the detailed rotational branching accompanying collision-induced electronic state changes. Somewhat in contrast to the confused vibrational picture, there is a fairly common tendency to observe relatively small changes in rotational state. This is true for systems as diverse as N_2^+ $A\,^2\Pi_u$–$X\,^2\Sigma_g^+$ [16,17]; CN $A\,^2\Pi$–$X\,^2\Sigma^+$ and $A\,^2\Pi$–$B\,^2\Sigma^+$ [18–22]; N_2 $a\,^1\Pi_g$–$a'\,^1\Sigma_u^-$ [23]; CO^+ $A\,^2\Pi$–$X\,^2\Sigma^+$ [24]; Na_2 $B\,^1\Pi_u$–$(2)^1\Sigma_g^+$ [25,26]; K_2 $^1\Delta_g$–$^1\Sigma_g^+$ [27]; and I_2 $E(0_g^+)$–$D(0_u^+)$ [28].

---

* Corresponding author.

SSDI 0009-2614(95)00798-9

The subject of this Letter is an extension of previous work on vibrational state-specific energy transfer between analogous excited $^2\Delta$ and $^2\Sigma^+$ states in the silicon halides, SiCl [14,15] and, more particularly, SiF [29]. The first partially rotationally resolved results for SiF C $^2\Delta$–B $^2\Sigma^+$ transfer in collisions with H_2 and (in less detail) N_2 are reported. We discuss whether these observations are consistent with the impulsive mechanism previously proposed to explain the vibrational branching ratios [29].

2. Experimental

The apparatus has essentially been described previously [15,29], although some details of the laser system and detection electronics have subsequently been modified.

Ground state SiF X $^2\Pi$ radicals were generated by microwave discharge of an SiF_4/Ar mixture in a discharge-flow system. A second flow of the quenching gas (H_2 or N_2) was added downstream. The total pressure was maintained at typically a few Torr by a mechanical pump (Alcatel 2063, or, latterly, Edwards E2M80).

Laser-induced fluorescence (LIF) was excited downstream of the mixing point by a frequency-doubled dye laser (Spectron SL4000D-FM4A) pumped by the 355 nm harmonic of a Nd:YAG laser (Spectron SL803). The fluorescence was dispersed (Hilger and Watts, Monospek 1000, 1 m monochromator), detected (EMI 9558QB photomultiplier), preamplified (EMI A2, fast 10 × amplifier) and captured (Transiac 2001A transient digitiser, 100 MHz bandwidth, 10 ns interval). The experiment was controlled by a personal computer via a CAMAC (IEEE 583) databus and associated modules.

Gases were used directly as supplied and had the following stated purities: SiF_4 (Union Carbide, 99.99%), Ar (BOC, 99.99%), H_2 (BOC, 99.99%), N_2 (BOC, 99.998%).

3. Results

3.1. Rotationally selective excitation of SiF C $^2\Delta$

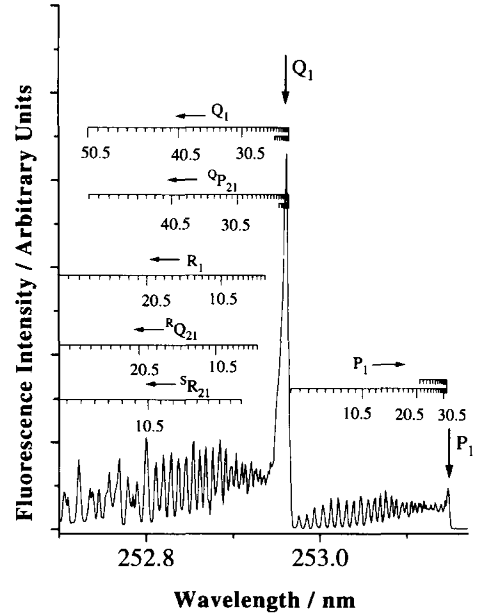

Fig. 1. LIF excitation spectrum of the SiF C $^2\Delta$–X $^2\Pi_{1/2}$ (0, 0) sub-band. The 'Q_1' and 'P_1' features referred to in the text are indicated by arrows.

Fig. 1 shows a LIF excitation spectrum of the $^2\Delta$–$^2\Pi_{1/2}$ sub-band of the C–X (0, 0) transition [30]. The most significant features for the present study are the two heads which form at approximately 252.95 and 253.15 nm, respectively. In fact, the feature labelled 'Q_1' in Fig. 1 is more correctly the combination of the Q_1 and $^QP_{21}$ heads, but these nevertheless form at similar J values of around 12.5. In contrast, the 'P_1' head, which is due to a single spectroscopic branch (apart from the unresolved Λ-doubling of all lines), forms at a much higher J of around 34.5. In this initial exploratory investigation, we therefore had a convenient, if admittedly imperfectly resolved, way of preparing distinct rotational populations in the C $^2\Delta$ state while retaining the relatively large signals associated with pumping at the bandheads.

3.2. Time-averaged rotational populations in the C $^2\Delta$ state

It is not entirely straightforward to predict the time-averaged rotational populations following excitation at either of the bandheads. We have instead quantified them more directly by dispersing the C $^2\Delta$–X $^2\Pi$ fluorescence. Because of the spin–orbit splitting in the $X\,^2\Pi$ state, the highest probability C–X (0, 0) band can conveniently be used for both excitation ($C\,^2\Delta$–$X\,^2\Pi_{1/2}$) and detection ($C\,^2\Delta$–$X\,^2\Pi_{3/2}$).

Such fluorescence spectra are shown in Fig. 2. Signal was collected over the full range of the fluorescence decay (approximately 400 ns, about four times the $C\,^2\Delta$ state radiative lifetime of 94 ± 2 ns [29]). It is obvious that the rotational contours in the spectra following Q_1 and P_1 pumping are distinctly different.

The $C\,^2\Delta$ state rotational distributions were extracted by an iterative fitting procedure, making use of the known spectroscopy of the C–X system [30]. An interesting subtlety arises because P_1 excitation unambiguously populates only the $\Omega = 3/2$ spin–orbit component in the $C\,^2\Delta$ state, whereas 'Q_1' pumping (see above) produces a mixture of $\Omega = 3/2$ and $5/2$ levels. It was also quickly established that some collisional mixing of the 3/2 and 5/2 levels was competitive with emission. The time-averaged ratio was therefore treated as an adjustable parameter in the fit. Not surprisingly, this ratio was found to be around unity following (partially saturated) Q_1 excitation, but nearer to 3.5 : 1 in favour of the initially populated 3/2 level for P_1 pumping.

Of more primary interest were the J' populations, which were determined by iteratively adjusting smoothly varying distributions to obtain the best visual agreement with the experimental contours. Because of the limited experimental resolution the resulting individual rotational populations are certainly not unique, but characteristics such as the location of the peak of the distribution and the limits on population in the upper and lower extremes are quite well established.

The 'best-fit' spectra are compared with experiment in Fig. 2. (It is probable that the level of agreement could be further improved by allowing different J' population distributions in the $\Omega = 3/2$ and 5/2 levels.) The corresponding distributions are plotted in Fig. 3 (closed symbols). Partial collisional rotational redistribution has apparently competed with

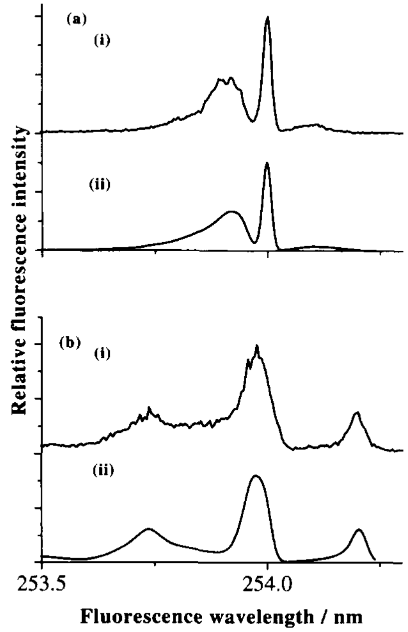

Fig. 2. Dispersed fluorescence spectra of the SiF $C\,^2\Delta$–$X\,^2\Pi_{3/2}$ (0, 0) sub-band following excitation on the $C\,^2\Delta$–$X\,^2\Pi_{1/2}$ sub-band. (a) Q_1 excitation (observed with bandwidth 3.1 cm^{-1}); (b) P_1 excitation (bandwidth 4.7 cm^{-1}). In each case, (i) experimental spectrum (total pressure 2.5 Torr); (ii) best-fit simulation as described in the text.

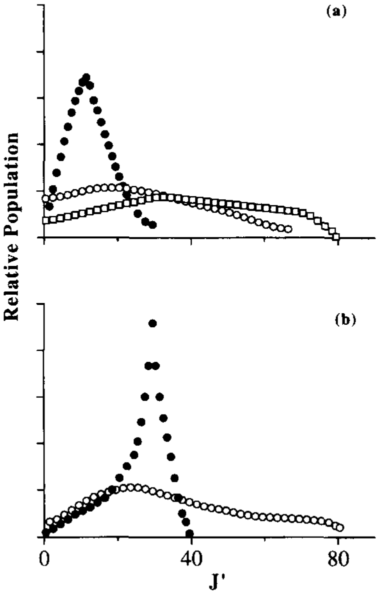

Fig. 3. Rotational populations derived from simulations of dispersed fluorescence spectra. (a) Q_1 excitation; (b) P_1 excitation. Distributions (normalised to the same total population): directly excited SiF $C\,^2\Delta$, $v' = 0$ (●); collisionally populated SiF $B\,^2\Sigma^+$, $v' = 0$, with (○) 1 Torr H_2 + 1.5 Torr Ar, and (□) 1 Torr N_2 + 1.5 Torr Ar.

emission, but thermalisation is very far from complete. Indistinguishable C $^2\Delta$ state distributions were obtained with or without H_2 quencher at comparable total pressures.

3.3. Product rotational populations in the B $^2\Sigma^+$ state

It is important to stress that, as in our our earlier work [29], the much shorter radiative lifetime of the B $^2\Sigma^+$ state ($< \approx 10$ ns) ensures that any *secondary* collisional redistribution of the B $^2\Sigma^+$ state rotational population would be comfortably exceeded by the width of the initial C state distribution. Therefore, collision-induced B–X fluorescence spectra are a good measure of the *nascent* B $^2\Sigma^+$ state rotational populations.

The dominant vibrational channel in collisional transfer from C $^2\Delta$, $v = 0$ is B $^2\Sigma^+$, $v' = 0$, for all successful quenchers [29]. Furthermore, the B–X (1, 1) and (2, 2) bands are relatively weak through having poor Franck–Condon overlap [30]. Therefore, the collision-induced B–X emission in the vicinity of 286–290 nm is almost completely dominated by the (0, 0) band.

Dispersed, collision-induced B–X (0, 0) fluorescence spectra in the presence of H_2 are presented in Fig. 4. Signal was again collected over the full range of the fluorescence decay (400 ns gate), with the time-dependence of the B–X emission being controlled by the C $^2\Delta$ state lifetime. The P_1-excited spectrum appears to be qualitatively 'hotter' than the Q_1 spectrum. Also shown for comparison is the Q_1 spectrum with N_2 quencher. Although the signal-to-noise is inferior, the B $^2\Sigma^+$ state distribution is clearly more rotationally excited than the corresponding result for H_2.

These observations were quantified by a similar iterative fitting procedure to that used for the C–X fluorescence spectra. The resulting best-fit spectra are shown in Fig. 4, and the corresponding rotational distributions included in Fig. 3 (open symbols).

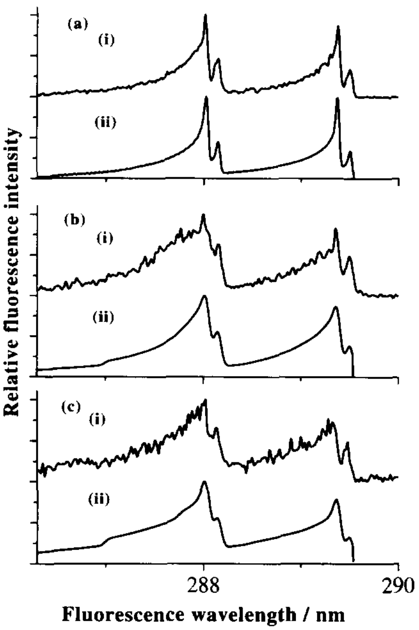

Fig. 4. Collisionally produced SiF B–X (0, 0) emission spectra. (a) Q_1 excitation, 1 Torr H_2 + 1.5 Torr Ar (bandwidth 4.7 cm^{-1}); (b) P_1 excitation, 1 Torr H_2 + 1.5 Torr Ar (bandwidth 9.4 cm^{-1}); (c) Q_1 excitation, 1 Torr N_2 + 1.5 Torr Ar (bandwidth 4.7 cm^{-1}). In each case: (i) experiment; (ii) simulation.

4. Discussion

Our principal observation is that a quite considerable fraction of the available energy is released as SiF product rotation in all the cases examined here. The relevant energy gaps are indicated in Fig. 5. Estimates of the average increases in the SiF rotational quantum number, δj, and the corresponding increases in rotational energy, δR, are listed in Table 1. Maximum values are also given, on the assumption that the highest levels in the product are likely to have come from the highest initial levels.

As noted in Section 1, this behaviour is unusual, because most other studies have revealed propensites for relatively small δj values [16–28]. These observations have been justified at various levels of theory, ranging from alternative limiting models [26] to more rigorous scattering calculations using realistic potentials [32–34]. A notable exception is the high rotational 'temperatures' reported for NH C $^1\Pi$–A $^3\Pi$ transfer induced by a variety of partners [8], although the authors did not present any arguments to explain these results.

For those quenchers which are effective in promoting SiF C $^2\Delta$ to B $^2\Sigma^+$ transfer (H_2, N_2, and

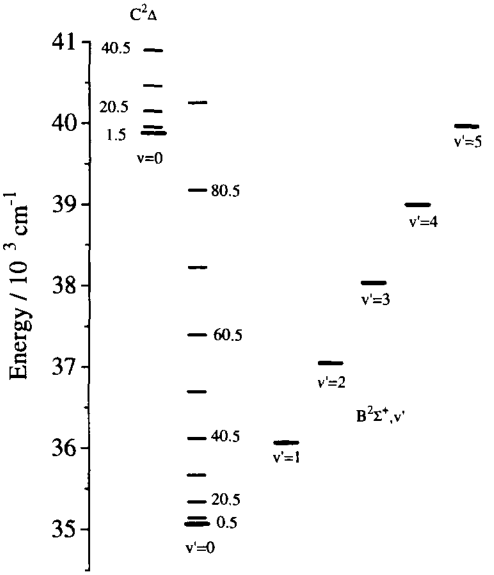

Fig. 5. Energy level diagram for selected SiF $C\,^2\Delta$ and $B\,^2\Sigma^+$ levels. Rotational spacings are indicated for the $C\,^2\Delta$, $v'=0$ and $B\,^2\Sigma^+$, $v'=0$ levels relevant to this study.

CH_4 of those examined), the distribution between vibrational levels has been shown to match closely the Franck–Condon overlap [29]. This is despite the surprisingly large vibronic energy gaps of around 5000 cm^{-1} which are involved (see Fig. 5): starting from $C\,^2\Delta$ $v'=0$ and 1, the $\Delta v = 0$ channels were found to be most probable. Essentially no population was deposited in the higher, more vibronically isoenergetic $B\,^2\Sigma^+$ state levels.

We have argued [29] that this is indicative of a 'sudden', impulsive mechanism, and is consistent with the accepted electronic characters of the two states. The $C\,^2\Delta$ state is an excited valence state, but the $B\,^2\Sigma^+$ state is a Rydberg state with an outer electron occupying a much greater volume. It is therefore reasonable that there could be a much greater SiF...quencher repulsion at the intermolecular distance at which the $C\,^2\Delta$–$B\,^2\Sigma^+$ transition is induced.

At first sight, kinematic factors, particularly for H_2, might appear to be counter to the observed partitioning of such a significant fraction of the available energy to SiF rotation through a purely impulsive mechanism. However, we now briefly describe a limiting model which dispels such a conclusion.

The SiF $B\,^2\Sigma^+$ state molecule is considered, at the instant of its production from the $C\,^2\Delta$ state, as a 'hard-shape' interacting with a 'hard-sphere' quencher molecule. The most important feature of the hard-shape is the point on the surface for which the extrapolated normal corresponds to the largest impact parameter, b_{max} [31]. An impulse imparts the largest possible torque to the hard-shape if it is along this normal.

The value of δj_{max} in the simpler case of a collision in which there is *no* conversion of electronic potential to kinetic energy is well known [31]. This maximum results from coplanar collisions with the initial orbital angular momentum, l_i, parallel to the initial rotational angular momentum, j_i. We have extended the analysis by further assuming that at the point of impact an additional instantaneous impulse

Table 1
Mean and maximum properties [a] of initial $C\,^2\Delta$, $v'=0$ and product $B\,^2\Sigma^+$, $v'=0$ rotational distributions

Excitation	j_i [b]		Quencher	j_f [c]		δj [d]		δR [e]	
	mean	max		mean	max	mean	max [f]	mean	max [f]
Q_1	12.5(2)	31.5(3)	H_2	27.5(2)	67.5(3)	15(3)	36(4)	540(80)	2300(300)
			N_2	38.5(3)	79.5(6)	26(4)	48(7)	1080(150)	3400(600)
P_1	25.5(3)	39.5(3)	H_2	35.5(3)	80.5(5)	10(4)	41(6)	600(150)	3100(600)

[a] Numbers in parentheses represent estimated uncertainties, assessed visually from the sensitivity of the fit to the trial distribution.
[b] Initial rotational quantum number (nearest half integer).
[c] Product rotational quantum number (nearest half integer).
[d] Increase in rotational quantum number.
[e] Increase in rotational energy/cm^{-1}.
[f] Assuming j_f(max) produced from j_i(max).

is imparted, releasing an energy, ΔE. Total energy conservation now requires that

$$p_f^2/2\mu + \hbar^2 j_f^2/2I = p_i^2/2\mu + \hbar^2 j_i^2/2I + \Delta E, \tag{1}$$

where p is the linear momentum and the subscripts i and f indicate initial and final values, respectively. I is the moment of inertia of the hard-shape and μ is the reduced mass of the pair which collide with centre-of-mass velocity, v_{rel}. When combined with conservation of total angular momentum, the solution for $\delta j_{\max}$ is the (more positive) root of a quadratic,

$$\delta j_{\max} = b_{\max}/[\hbar(1+\eta)] \times \left\{ \alpha + \left[\alpha^2 + 2\mu \Delta E (1+\eta) \right]^{1/2} \right\}, \tag{2a}$$

with

$$\eta = \mu b_{\max}^2 / I \tag{2b}$$

and

$$\alpha = p_i - \hbar \mu b_{\max} j_i / I. \tag{2c}$$

We have explored the consequences of this result for H_2...SiF collisions. The most unknown quantity is $b_{\max}$ (note that it is not simply related to the magnitude of the cross section for the collisional transfer process). However, it seems unlikely, on intuitive physical grounds, to be greater than the distance (0.92 Å) between the F nucleus and the SiF centre-of-mass. In other words, the force acting locally on the H_2 is unlikely to be directed from a point on the rotor axis which lies beyond the F atom. Taking this distance for $b_{\max}$, upper limiting $\delta j_{\max}$ values of around 35 to 40 necessary to match the H_2 experiments (see Table 1) require v_{rel} values of 4000 to 5500 ms^{-1}. These velocities correspond to the high velocity tail of a 300 K thermal distribution, being exceeded in approximately 1.5 and 0.01% of collisions, respectively.

The calculations highlight the approximate additivity of the contributions to j_f from j_i, from the impulsive conversion of l_i to j_f, and from the additional impulse ΔE. We conclude that the observed values of $\delta j_{\max}$ *are* compatible with a purely repulsive interaction, although it admittedly requires contributions which are towards the upper end of the expected ranges from each of the sources. We suggest that the increase in average and maximum final rotational level with a shift in the initial distribution to higher levels (comparison of Q_1 and P_1 pumping) is further supporting evidence for a repulsive interaction. The model also successfully predicts readily, on kinematic grounds, that the degree of SiF product rotational excitation should be higher for N_2 than for H_2. We are cautious not to attach too much physical significance to the detailed predictions of this limiting model. Nevertheless, even the raw rotational results themselves indicate that there must be a substantial non-spherical component to the SiF...quencher potential.

An interesting alternative suggestion is that some collisions would lead to transient complexes because the Rydberg electron would penetrate beyond an effective SiF^+...quencher core which was quasi-bound by charge-induced dipole forces. This might provide an efficient mechanism for the conversion of orbital to product rotational angular momentum. Nevertheless, it is clear that there must still be conversion to SiF rotation of a considerable fraction of the electronic potential energy which is released. Any such bound potential would therefore have to be substantially anisotropic in its exit channel. The involvement of a more strongly bound intermediate in which there was efficient coupling between motion in the SiF internal and intermolecular coordinates would seem to be precluded by the observed Franck–Condon control of the product *vibrational* distribution [29].

We are currently refining our experimental technique for the study of the SiF $C\,^2\Delta - B\,^2\Sigma^+$ system by employing single rotational level excitation and time-gating the fluorescence emission. This should allow the j_i-dependent distribution of δj values to be measured more precisely. More details of our model calculations will be reported in conjunction with such results. We are sure, however, that the present measurements have clearly demonstrated the unusually large rotational energy release associated with this process.

Acknowledgements

We are grateful to Dr. K.P. Lawley for several helpful discussions. Mr. C.J. Randall and Ms. A.

Chow were involved in some aspects of the experimental procedure. We thank the EPSRC for an equipment grant (GR/J29657) and for providing studentships for CW and NJ.

References

[1] D.H. Katayama, J. Chem. Phys. 81 (1984) 3495.
[2] D.H. Katayama, A.V. Dentamaro and J.A. Welsh, J. Chem. Phys. 87 (1987) 6983.
[3] D.H. Katayama and A.V. Dentamaro, J. Chem. Phys. 91 (1989) 4571.
[4] A. Rotem and S. Rosenwaks, Opt. Eng. 22 (1983) 564.
[5] N.L. Garland and D.R. Crosley, Appl. Opt. 24 (1985) 4229.
[6] K.J. Rensberger, M.J. Dyer and R.A. Copeland, Appl. Opt. 27 (1988) 3679.
[7] D.R. Crosley, R.A. Copeland and J.B. Jeffries, State-specific energy transfer in diatomic radicals, SRI Report MP88-025 (1988).
[8] F. Rohrer and F. Stuhl, J. Chem. Phys. 86 (1987) 226.
[9] H.H. Nelson and J.R. McDonald, J. Chem. Phys. 93 (1990) 8777.
[10] J.S. Adams and L. Pasternack, J. Phys. Chem. 95 (1991) 2975.
[11] J. Wildt, G. Bednarek and E.H. Fink, Chem. Phys. 122 (1988) 463.
[12] I.J. Wysong, J.B. Jeffries and D.R. Crosley, J. Chem. Phys. 91 (1989) 5343.
[13] Ch. Ottinger and A.F. Vilesov, J. Chem. Phys. 100 (1994) 1805.
[14] J.B. Jeffries, J. Chem. Phys. 95 (1991) 1628.
[15] S. Singleton and K.G. McKendrick, J. Phys. Chem. 97 (1993) 1389.
[16] D.H. Katayama, Phys. Rev. Letters 54 (1985) 657.
[17] D.H. Katayama and A.V. Dentamaro, J. Chem. Phys. 85 (1986) 2595.
[18] N. Furio, A. Ali and P.J. Dagdigian, J. Chem. Phys. 85 (1986) 3860.
[19] G Jihua, A. Ali and P.J. Dagdigian, J. Chem. Phys. 85 (1986) 7098.
[20] A. Ali, G Jihua and P.J. Dagdigian, J. Chem. Phys. 87 (1987) 2045.
[21] P.J. Dagdigian, D. Patel-Misra, A. Berning, H.-J. Werner, M.H. Alexander, J. Chem. Phys. 98 (1993) 8580.
[22] A. Ali, G Jihua and P.J. Dagdigian, Chem. Phys. Letters 131 (1986) 331.
[23] D.H. Katayama and A.V. Dentamaro, J. Chem. Phys. 97 (1992) 2820.
[24] A.V. Dentamaro and D.H. Katayama, J. Chem. Phys. 90 (1989) 91.
[25] K. Hussein, M. Aubert-Frecon, O. Babaky, J. D'Incan, C. Effantin and J. Verges, J. Mol. Spectry. 114 (1985) 105.
[26] A.G Astill.A.J. McCaffery, S.C. Taylor, B.J. Whitaker and M.J. Wynn, J. Chem. Phys. 89 (1989) 184.
[27] L. Li, A.M. Lyyra, H. Wang and W.C. Stwalley, Chem. Phys. Letters 179 (1991) 417.
[28] W. Ubachs, I. Aben, J.B. Milan, G.J. Somsen, A.G. Stuiver and W. Hogervorst, Chem. Phys. 174 (1993) 285.
[29] C.W. Watson and K.G. McKendrick, Chem. Phys. 187 (1994) 79.
[30] C.W. Watson and K.G. McKendrick, Chem. Phys. 187 (1994) 87.
[31] J.N. Murrell and S.D. Bosanac, Introduction to the theory of atomic and molecular collisions (Wiley, New York, 1989) p. 79.
[32] M.H. Alexander and G.C. Corey, J. Chem. Phys. 84 (1986) 100.
[33] H.-J. Werner, B. Follmeg and M.H. Alexander, J. Chem. Phys. 89 (1988) 3139.
[34] H.-J. Werner, B. Follmeg, M.H. Alexander and D. Lemoine, J. Chem. Phys. 91 (1989) 5425.